Experiments and modeling of electron-transfer of DIRB

James Kubicki[A], Brendan Puls[A], Yufeng Qian[B] and Ming Tien[B]

[A]Department of Geosciences, The Pennsylvania State University, University Park, PA, USA, Email jdk7@psu.edu
[B]Department of Biochemistry & Molecular Biology, The Pennsylvania State University, University Park, PA, USA, Email mxt3@psu.edu

Abstract
We use quantum chemical calculations and experimental data to describe the structures and functions of mediator molecules used in the terminal electron transfer step of dissimilatory iron-reducing bacteria (DIRB). Mediator molecules increase the rate of electron transfer by either chelating reducible iron (Fe^{3+}) or shuttling electrons between outer-membrane cytochromes and iron-oxide minerals. Examples of mediator molecules examined in recent literature include ethylenediaminetetraacetic acid (EDTA) (Wang *et al.* 2008), citric acid (Wang *et al.* 2008), riboflavin (Canstein *et al.* 2008), flavin mononucleotide (FMN) (Canstein *et al.* 2008), menaquinone (Newman and Kolter 2000), and anthraquinone disulfonate (AQDS) (Lovley *et al.* 1998). Focusing on several of these mediator molecules, our goals are to 1) determine the potential for each mediator to chelate reducible iron and 2) determine the potential for each mediator to shuttle electrons. We use UV/Vis spectroscopy to measure the electronic spectra and quantum chemistry to calculate the minimum energies of each mediator in four states: 1) oxidized, 2) reduced, 3) bound to reducible iron (Fe^{3+}), and 4) bound to reduced iron (Fe^{2+}). We determine the potential for each mediator to chelate reducible iron or shuttle electrons by comparing the measured spectra and calculated minimum energies. As a future part of this study, we plan to explore the function of the mediator molecules as iron chelators by measuring binding constants for each mediator with reducible iron (Fe^{3+}) and reduced iron (Fe^{2+}) using isothermal titration calorimetry (ITC). This study is conceived as the first step towards characterizing the role of microbial iron reduction mediators on a molecular level. The next step will be to characterize the interactions of the mediator molecules with the electron donor (outer-membrane cytochromes) and the electron acceptor (iron-oxide minerals) of the terminal electron transfer step of microbial iron reduction.

Key Words
Quantum- mechanical, electron-transfer, flavin, iron-oxide

Introduction
Recent research on the reduction of iron by DIRB has focused on determining how its rate and long-term extent are controlled in natural environments. In a study of the reduction of Fe-oxyhydroxide minerals with a wide range of specific surface areas, crystallographic structures, and thermodynamic properties by DIRB, Roden (2006) found that the rate and long-term extent of reduction are strictly limited by access to the substrate. The interfacial rate-limiting reaction, however, has not yet been characterized on a molecular level (Frederickson *et al.* 2008). Research has revealed three methods of substrate access by DIRB: 1) direct adhesion to insoluble substrates (Caccavo and Das 2002), 2) reduction of soluble electron shuttles (Newman and Kolter 2000), and 3) reduction of soluble metal chelates (Nevin *et al.* 2002). In most natural systems where direct access to Fe-oxyhydroxide minerals is limited or where DIRB cells grow in biofilms, the presence of soluble electron shuttles or metal chelates increases the bioavailability of reducible iron and consequently the rate of microbial iron reduction (Nevin *et al.* 2002). Bioremediation systems based on the stimulation of DIRB growth and activity can therefore use the addition of soluble substrates to promote microbial iron reduction.

Methods
Experimental
UV/Vis spectra were measured for 1) flavin mononucleotide (FMN), 2) riboflavin (RBF), 3) $FeCl_3$, 4) FMN mixed with $FeCl_3$, and 5) RBF mixed with $FeCl_3$. All species were dissolved at 100 μM and adjusted to pH 7 with NaOH or HCl. No buffer was added to avoid unwanted interactions. Peaks were selected at the local maxima of the spectra with no other curve fitting. UV/Vis spectra were measured over the range of 200 to 800 nm at a resolution of 0.1 nm. The background was measured prior to solution measurement and subtracted from each of the solution spectra. All solutions were measured with a dual beam relative to a blank which contained distilled water. Difference spectra were calculated by subtracting the mixed

FMN/$FeCl_3$ and RBF/$FeCl_3$ solutions from the sums of the the FMN and $FeCl_3$ solutions and RBF and $FeCl_3$ solutions, respectively.

Computational
Gas-phase structures were optimized using Gaussian 03. The calculations were perfomed using the Becke 3-parameter exchange functional and the Lee-Yang-Parr correlation functional (B3LYP) using the 6-311G(d,p) basis set. Vibrational frequency calculations were performed for each of the optimized structures to verify that these were true minima and to estimate Gibbs free energies. Using the optimized structures, UV/Vis peaks were calculated using time-dependant density functional theory (TD-DFT). Peaks were calculated seperately for singlet and triplet electronic transitions over the UV/Vis range to compare to experimental measurements. Free energies were calculated using the gas-phase optimized and frequency-corrected energies for the individual species and adjusting for stoichiometry. Changes in free energy upon binding were calculated by subtracting the energies of the FMN, RBF, and Fe^{3+} monomers from the energies of the FMN/Fe^{3+} and RBF/Fe^{3+} complexes. Several configurations for FMN/Fe^{3+} and RBF/Fe^{3+} complexes were used to achieve theoretical binding structures. The comparison of the calculated peaks for the theoretical binding structures to the measured UV/Vis peaks is a test of the validity of the theoretical structures.

Results

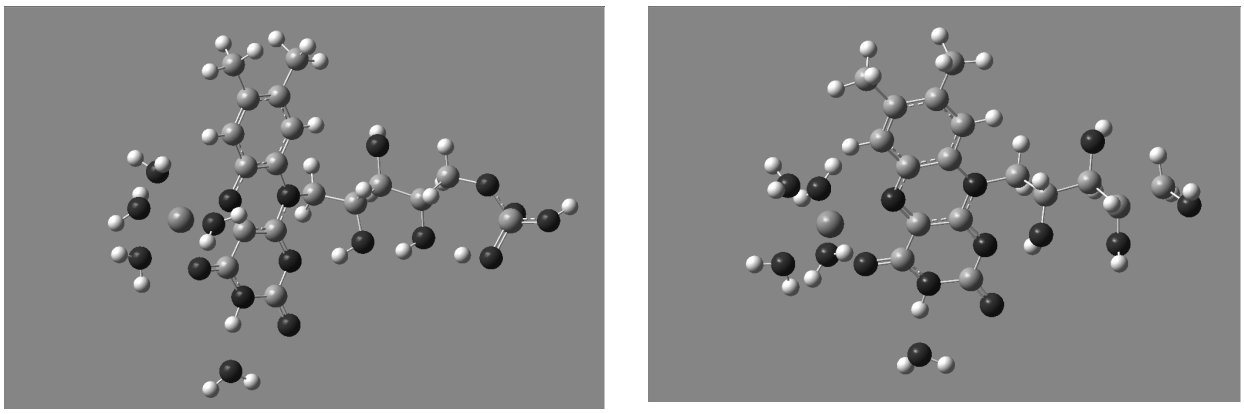

Figure 1. Gas-phase optimized structures for example configurations of FMN/Fe^{3+} (left) and RBF/Fe^{3+} (right). All calculations done using the Gaussian 03 (B3LYP 6-311G(d,p)).

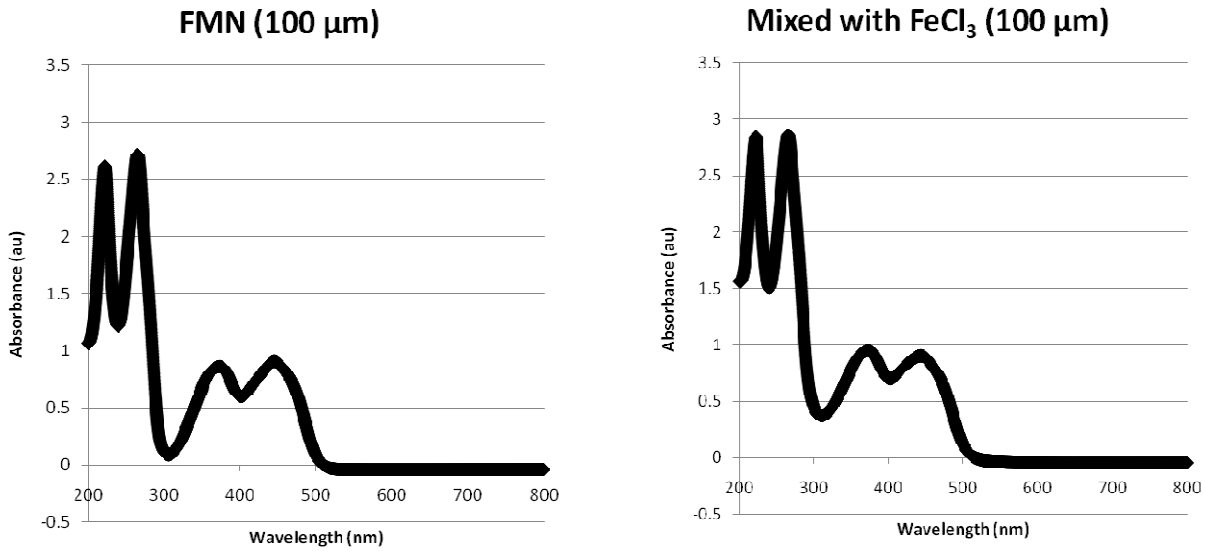

Figure 2. UV/Vis spectra for FMN (left) and FMN/Fe^{3+} (right). All dissolved species at 100 µM and pH 7.

Table 1. Wavelengths (nm) and intensities (au) of measured UV/Vis peaks for FMN, FMN/Fe^{3+}, RBF, and RBF/Fe^{3+}. All dissolved species at 100 µM and pH 7.

Spectrum	Peak #1	Peak #2	Peak #3	Peak #4
FMN	222.3 nm	265.2 nm	373.1 nm	445.1 nm
(100 µL)	2.616 au	2.717 au	0.865 au	0.905 au
Mixed with $FeCl_3$	221.1 nm	265.7 nm	373.0 nm	443.1 nm
(100 µL)	2.844 au	2.863 au	0.954 au	0.907 au
RBF	219.8 nm	261.6 nm	371.1 nm	(none)
(100 µL)	2.703 au	2.673 au	0.810 au	
Mixed with $FeCl_3$	219.5 nm	261.8 nm	356.3 nm	(none)
(100 µL)	2.994 au	2.865 au	0.942 au	

Table 2. Wavelengths (nm) and intensities (au/f-values) of measured and calculated UV/Vis peaks for FMN and RBF. All species at 100 µM and pH 7. Calculations done using the Gaussian 03 (TD-DFT B3LYP 6-311G(d,p)).

Spectrum	Peak #1	Peak #2	Peak #3	Peak #4
Measured FMN	222.3 nm	265.2 nm	373.1 nm	445.1 nm
(100 µL)	2.616 au	2.717 au	0.865 au	0.905 au
Calculated FMN	217.1 nm	252.8 nm	333.0 nm	405.0 nm
(N/A)	(0.3740)	(0.3015)	(0.1854)	(0.1300)
Measured RBF	219.8 nm	261.6 nm	371.1 nm	(none)
(100 µL)	2.703 au	2.673 au	0.810 au	
Calculated RBF	216.1 nm	253.6 nm	332.8 nm	(none)
(N/A)	(0.1702)	(0.3762)	(0.1668)	

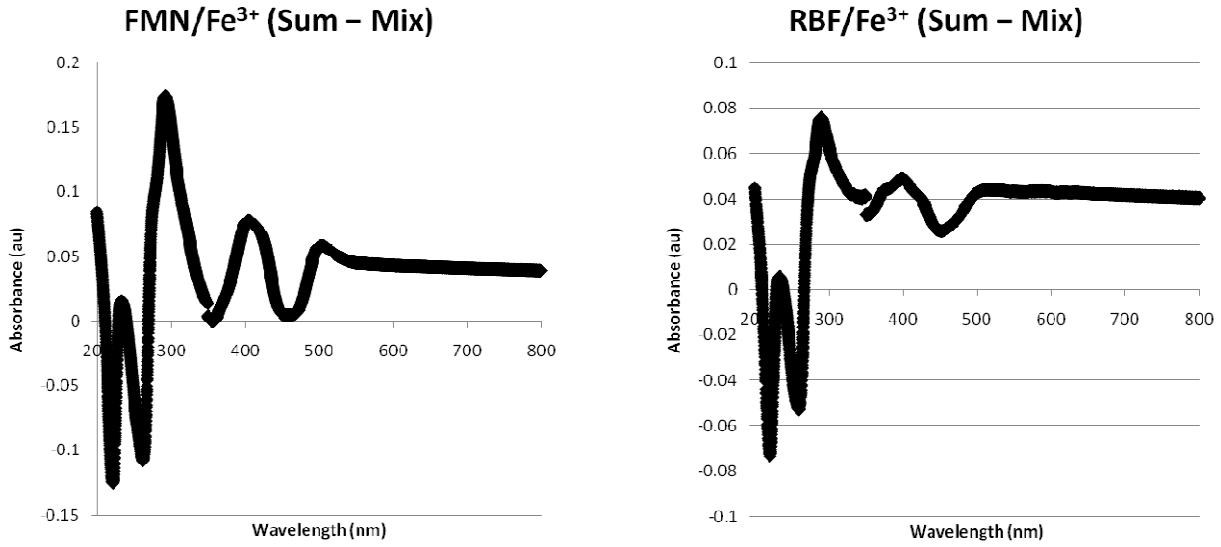

Figure 3. Difference spectra for FMN/Fe^{3+} (left) and RBF/Fe^{3+} (right). All dissolved species at 100 µM and pH 7.

Conclusions

UV/Vis spectra were measured for 1) FMN, 2) RBF, 3) FMN mixed with $FeCl_3$, and 4) RBF mixed with $FeCl_3$. Based on the measured spectra, peak shifts upon mixing with $FeCl_3$ are within 2 nm. This may be interpreted as a sign of weak or absent binding. However, the spectra do exhibit significant changes in the absorbance. Absorbance changes may indicate a binding event. Absorbance changes measured during a UV/Vis titration can indicate the strength of the binding. Peaks were calculated for FMN and RBF. Calculated peaks appear to be shifted down from measured peaks. However, the calculated peaks were based on gas-phase optimized structures that do not account for solvent. Calculated absorbance values appear to scale roughly with the measured absorbance values. Reoptimization of the gas-phase structures with a continuum solvent model may correct the down-shifted peaks. In addition, energy calculations for the solvent-optimized structures will show differences in stability among the several configurations tested. Repeating the calculations with Fe^{2+} will allow comparison of energy changes upon binding among the theoretical configurations. Based on the gas-phase optimizations, changes in free energy are expected to be negative upon binding. This indicates that binding is thermodynamically favored. For FMN, the change in free energy for the binding is lower for the configuration with Fe^{3+} bound to the phosphate group than for the

configuration with Fe^{3+} bound to the isoalloxazine unit. This may indicate that binding to the phosphate group is the favored configuration.

References

Caccavo F Jr, Das A (2002) Adhesion of dissimilatory Fe(III)-reducing bacteria to Fe(III) minerals. *Geomicrobiol. J.* **19,** 161–177

Canstein H Von, Ogawa J, Shimizu S, Lloyd JR (2008) Secretion of flavins by *Shewanella* species and their role in extracellular electron transfer. *Appl. Environ. Microbiol.* **74,** 615-623.

Fredrickson JK, Zachara JM (2008) Electron transfer at the microbe-mineral interface: A grand challenge in biogeochemistry. *Geobiol.* **6,** 245-253.

Lovley DR, Fraga JL, Blunt-Harris EL, Hayes LA, Phillips EJIP, Coates JD (1998) Humic substances as a mediator for microbially catalyzed iron reduction. *Acta Hydrochim. Hydrobiol.* **26,** 152-157.

Newman DK, Kolter R (2000) A role for excreted quinones in extracellular electron transfer. *Nature* **405,** 94-97.

Roden E (2006) Geochemical and microbiological controls on dissimilatory iron reduction. *C.R. Geosci.* **338,** 456-467.

Wang Z, Liu C, Wang X, Marshall MJ, Zachara JM, Rosso KM, Dupuis M, Fredrickson JK, Heald S, Shi L (2008) Kinetics of Reduction of Fe(III) Complexes by Outer Membrane Cytochromes MtrC and OmcA of Shewanella oneidensis MR-1. *Appl. Environ. Microbiol.* **74,** 6746-6755.